Semi-Automated Basal Ganglia Segmentation using Large Deformation Diffeomorphic Metric Mapping

Ali Khan†, Elizabeth Aylward*, Patrick Barta‡ and Michael Miller‡ and Mirza Faisal Beg†

Objective

Shape and volume change of the basal ganglia structures, which include the caudate nucleus and putamen, have been the focus of investigation in clinical studies of Huntington's Disease [1] and other neuro-degenerative disorders. Manual segmentation by a trained rater is the current anatomic gold standard, but this technique requires a sizable amount of time from an anatomic expert and suffers from inter-rater reliability issues. Reliable and accurate semi-automated segmentation of the caudate nucleus is limited by the following factors: limited resolution of MRI scans, inhomogeneous intensities throughout the caudate, and ill-defined boundaries.

We have developed the LDDMM tool [2], used for non-rigid registration of MRI images via intensity based matching. Given a template image, target image, and template segmentation, the non-rigid mapping of the template image to the target image can be used to propagate the template segmentation, generating a target segmentation.

Methods

Patient MR scans from three different clinical backgrounds were utilized in this study; 5 from patients with Huntington's disease (Series 1), 8 from pre-symptomatic carriers of the HD gene (Series 2), and 5 from individuals with no known caudate atrophy (Series 3).

Global alignment of the basal ganglia structures is required before intensity-based image matching can take place; rigid landmark-based registration was used to accomplish this task. We chose to place landmarks on the surfaces of the lateral ventricles because of their unique properties: adjacency to the caudate nucleus during all stages of atrophy, well-defined boundaries, and homogeneous intensities within these boundaries. The ventricle segmentation used for surface generation is produced by global thresholding with user guidance and takes a trained user approximately five minutes to complete. Ventricular surfaces are displayed below, showing adjacency to the caudates and landmark placement.

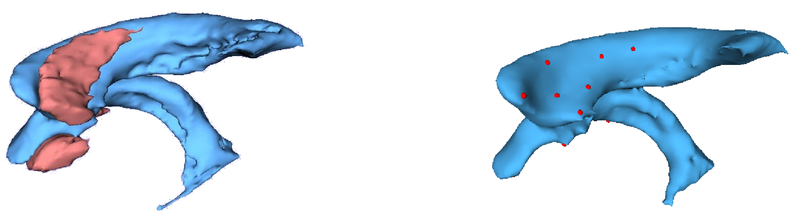

The images are cropped around the caudates, preprocessed for noise reduction using edge-preserving smoothing, and intensity normalized prior to input in the LDDMM program, which calculates the non-rigid mapping via intensity-based image matching. Image matching is achieved through the solution of the large deformations diffeomorphic metric mapping (LDDMM). Template and target images, I_0 and I_1, represented by functions $I : \Omega \rightarrow \mathbf{R}$, are mapped via the transformation $\varphi : \Omega \rightarrow \Omega$, where $\Omega \subseteq \mathbf{R}^3$. The diffeomorphic transformation generated is smooth and has a smooth inverse, hence, smoothness of anatomical features is preserved and coordinates are transformed consistently. An overview of our procedure is illustrated below.

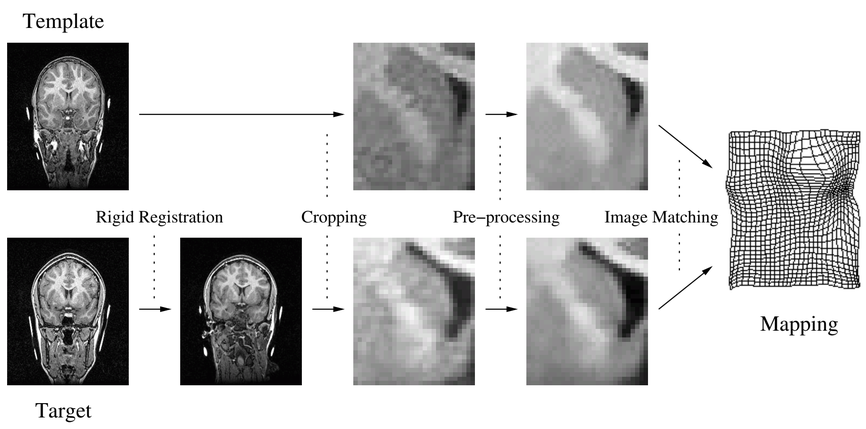

Results and Conclusion

To facilitate comparison of our continuous automated segmentations with the binary manual segmentations, the manual segmentations are slightly smoothed. The L1-distance between segmentations is reported as the L1 error, and caudate volumes are also computed. As an estimate of surface distance, the Hausdorff distance metric is used to calculate the maximum surface distance between two segmentations. Accuracy results are shown in the following table, with the average and standard deviation of each metric reported for each dataset series.

Error Metric	Series 1	Series 2	Series 3
Volume Error (%)	5.10 ± 3.60	8.08 ± 3.72	7.72 ± 6.18
L1 Error (%)	27.94 ± 6.51	36.21 ± 5.51	30.17 ± 6.99
95% Sym. Hausdorff (mm)	2.10 ± 0.98	2.27 ± 0.75	2.19 ± 0.70

We compare results we get from choosing different mapping strategies: rigid rotation/translation, intensity-based image matching with and without edge-preserving smoothing, and pure segmentational matching. L1 error and volume error results for these comparisons are shown in following figures.

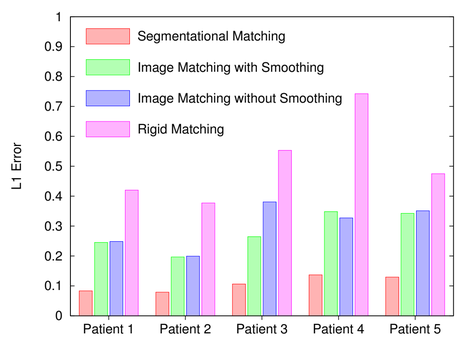

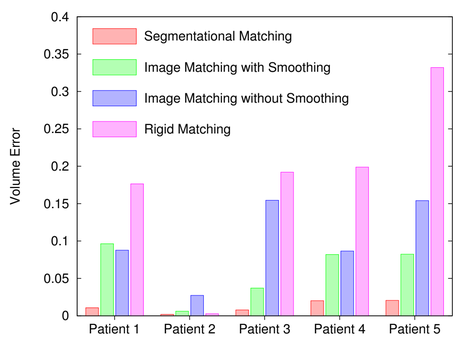

A comparison of automated and manual segmentations for two Series 1 patients is shown in the representative slices below. Automated segmentations are shown in blue with Patient A having L1 error = 26.45%, and Patient B having L1 error = 34.82%.

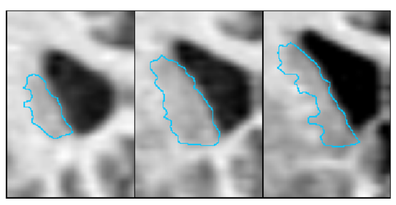

Patient A - automated segmentation

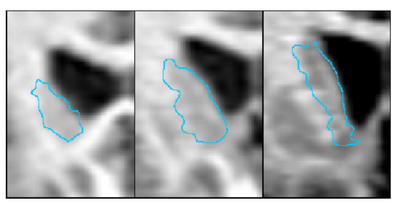

Patient B - automated segmentation

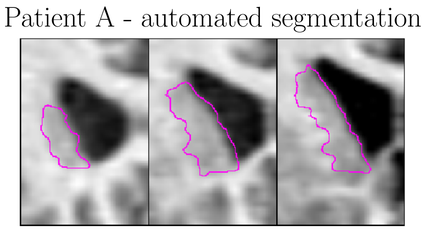

Patient A - manual segmentation

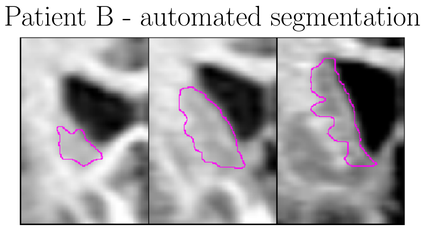

Patient B - manual segmentation

The automated and the manual segmentations are found to differ on the exterior boundary of the caudate. Due to the elongated, narrow shape of the caudate nucleus, the ratio of surface voxels to total voxels in the caudates is very high. Therefore, the partial volume effects are likely to be a heavy influence in calculation of the L1 distance. Examination of the above segmentations reveals that accurate delineation of the caudate nuclei is still present in segmentations possessing relatively high L1-distance errors.

Concluding, the results we have shown demonstrate that our semi-automated image matching system reliably segments the caudate nucleus with results comparable to currently existing semi-automated or automated methods. Segmentation of the basal ganglia via image matching is the initial step in shape analysis as the diffeomorphic mapping defines the necessary correspondence between images. Application of our procedure to other structures should also prove successful, as our findings indicate that the general image matching segmentation concept is robust.

References

[1] E.H. Aylward, A. Rosenblatt, K. Field, V. Yallapragada, K. Kieburtz, M. McDermott, L.A. Raymond, E.W. Almqvist, M. Hayden, and C.A. Ross. Caudate volume as an outcome measure in clinical trials for huntington's disease: a pilot study. *Brain Research Bulletin*, 62:137–141, 2003.

[2] M. Faisal Beg, Michael I. Miller, Alain Trouvé, and Laurent Younes. Computing large deformation metric mappings via geodesic flows of diffeomorphisms. *IJCV*, 61(2):139–157, February 2005.

† School of Engineering Science, Simon Fraser University, 8888 University Drive, Burnaby BC V5A 1S6, Canada
∗ Department of Radiology and Psychiatry, University of Washington, Box 357115, Seattle, WA 98195, USA
‡ Center for Imaging Science, The Johns Hopkins University, 301 Clark Hall, Baltimore, MD 21218, USA

School of Engineering Science, Simon Fraser University **http://www.sfu.ca/∼mfbeg**
Medical Image Analysis Lab, Simon Fraser University **http://mial.fas.sfu.ca/**

We acknowledge funding support from NSERC 31-611387 for this work.